Research Article | Vol. 27, No. 22 / 28 October 2019 / Optics Express 31290
Optics EXPRESS

# Bending and twisting effects on multicore fiber differential group delay

SERGI GARCÍA,* MARIO UREÑA, AND IVANA GASULLA

*ITEAM Research Institute, Universitat Politècnica de València, Camino de Vera, 46022 València, Spain*
*sergarc3@iteam.upv.es*

**Abstract:** In this paper we provide the theoretical and experimental evaluation of fiber bending and twisting effects on the group delay performance of a homogeneous 7-core fiber. We have experimentally evaluated the differential group delay between the central and outer cores for different curvature radii and twisting conditions, demonstrating that fiber twisting counteracts the degradation introduced by the curvature itself. These findings are generally applicable to time-sensitive application areas such as radio-over-fiber distribution and microwave photonics signal processing in fiber-wireless access networks, as well as high-capacity long-haul digital communications where digital multiple-input multiple-output processing may be required.



## 1. Introduction

Multicore fiber (MCF) transmission has been intensively investigated as an attractive technology for considerable enlargement of the fiber capacity beyond the Shannon capacity limit of optical networks, [1]. In addition to high-capacity digital communications, MCFs constitute a promising medium to develop interesting applications such as multi-parameter optical fiber sensing [2] and Microwave Photonics (MWP) signal processing [3]. One of the major physical impairments that could compromise the MCF performance in the above-mentioned areas of application relates to the existence of possible bending and twisting effects that may affect deployed fiber links. In the context of weakly MCFs, these detrimental effects have been studied mainly in relation to the fiber inter-core crosstalk considering both homogeneous and heterogeneous core configurations [4,5].

However, a variety of applications where time-delay control and synchronization play an important role require in addition a thorough analysis of the group delay performance of the different fiber cores. This is the case of radio-over-fiber transmission and signal processing in 5G (and beyond) fiber-wireless communications and MWP scenarios. Here, we include timing synchronization [6] of wireless signals in MCF-based radio access networks feeding multiple input multiple-output (MIMO) antenna systems [7]. Another representative scenario is reconfigurable microwave signal processing, where the radiofrequency (RF) signal is generated, modified or controlled by optical solutions based on incoherent discrete-time architectures [3]. In this regard, we have previously proposed the exploitation of both homogeneous and multicore fibers as a compact medium to provide different signal processing functionalities [8], including optical beamforming for wireless phased-array antennas [9], reconfigurable RF signal filtering [9] or multicavity optoelectronic oscillation [10].

The influence of fiber bending on the intercore differential group delay (DGD) have been previously addressed in [11] for a 10-km 4-core fiber link. There, the authors realized that the measured bending-induced DGD was lower than the one predicted from simulation, what they attributed to possible fiber twisting one will expect in a 10-km link. Nevertheless, this statement has not been corroborated by providing either the pertinent theory or the experimental demonstration for different levels of twisting and bending.

In this paper, we provide the theoretical and experimental evaluation of the effects of fiber bending and twisting on the group delay performance of a commercial homogeneous 7-core fiber

#374416 https://doi.org/10.1364/OE.27.031290
Journal © 2019 Received 2 Aug 2019; revised 28 Sep 2019; accepted 30 Sep 2019; published 14 Oct 2019

Optics EXPRESS

link. After providing the theoretical expressions for the computation of the DGD accumulated on a given fiber length for arbitrary bending and twisting conditions (as long as one assumes a constant twist rate along the fiber), we evaluate experimentally how the accumulated DGD is affected for different twisting scenarios applied to 25, 35 and 50-mm curvature radii. Finally, we experimentally demonstrate how these conditions reflect on the performance of a particular time-sensitive MWP signal processing functionality, microwave signal filtering, up to 50 GHz. All in all, we demonstrate how twisting actually counteracts the degradation introduced by the fiber curvature itself on the accumulated DGD.

## 2. Theoretical modeling

In general, a bent fiber core $m$ can be described as the corresponding straight core with an equivalent refractive index distribution $n_{eq,\,m}$, [12]:

$$n_{eq,\,m} = \left[n_m^2\left(1 + 2\frac{r_m}{R_b}\cos\theta_m\right)\right]^{1/2} \approx n_m\left(1 + \frac{r_m}{R_b}\cos\theta_m\right), \tag{1}$$

where $R_b$ is the bending radius, $n_m$ is the refractive index of core $m$ in the corresponding straight fiber and $(r_m,\theta_m)$ are the local polar coordinates of core $m$, as shown in Fig. 1(a).

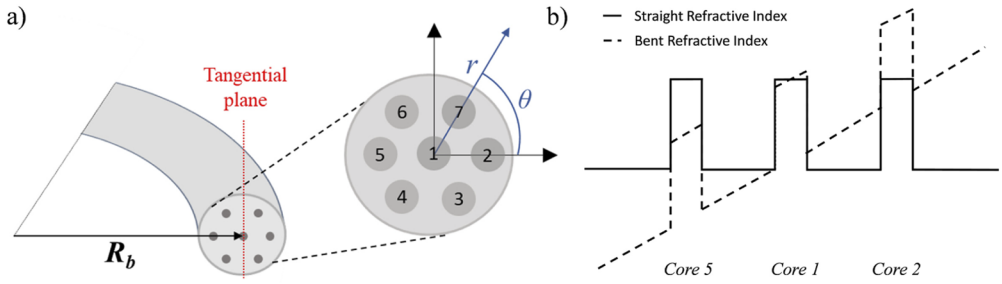


**Fig. 1.** Multicore fiber curvature with a bending radius $R_b$ and local polar coordinates $(r,\theta)$ indicated in the MCF cross section. (b) Effect of the fiber curvature on the refractive index profile of cores 1, 2 and 5 as compared to the straight condition.

Under the assumption of weak inter-core crosstalk, we can simplify the modal analysis and treat each core in isolation, without loss of generality. For a given core $m$, the propagation constant under bent condition (or equivalent propagation constant), $\beta_{eq,m}$, can be expressed as

$$\beta_{eq,\,m} = k_0 n_{eff_{eq,\,m}} = \sqrt{k_0^2 n_{eq,\,m}^2 - \frac{u_{eq}^2}{a_m{}^2}}, \tag{2}$$

where $a_m$ is the core radius, $k_0$ is the wavenumber, $n_{eff,eq,m}$ is the equivalent effective index and $u_{eq}$ is the normalized transverse propagation constant of the bent core, $u_{eq} = k_0\, a_m\, (n_{eq,m}{}^2 - n_{eff,eq,m}{}^2)^{1/2}$. In the case that the fiber core $m$ has a classic step-index profile, the parameter $u_{eq}$ is obtained by solving the well-known characteristic equation for step-index optical fibers, [13]. We can derive the equivalent group delay per unit length $(\tau_{eq,\,m}/L)$ from Eq. (2) as

$$\frac{\tau_{eq,\,m}}{L} = \frac{d\beta_{eq,\,m}}{d\omega} = \frac{1}{c\beta_{eq,\,m}}\left[k_0 n_{eq,\,m}^2 - 2\pi n_{eq,\,m}\frac{dn_{eq,\,m}}{d\lambda} + \frac{2\pi}{a_m^2 k_0^2}u_{eq}\frac{du_{eq}}{d\lambda}\right], \tag{3}$$

where $\omega$ is the optical angular frequency, $\lambda$ is the optical wavelength and $c$ is the light velocity in vacuum. We must note that Eqs. (2) and (3) are valid for any circular refractive index profile

Optics EXPRESS

distribution by using the proper characteristic equation to calculate the parameter $u_{eq}$, even considering multi-layer refractive profiles as derived in [14].

From Eq. (1), we see that the highest variation on the equivalent refractive index due to fiber curvatures occurs when the core forms an angle of $\theta = k\pi$, $k \epsilon$ Z, to the curvature plane. In addition, as Fig. 1(b) shows, the equivalent refractive indices of cores located in the 2nd and 3rd section quadrants decrease their values with respect to the equivalent straight fiber, while those located in the 1st and 4th quadrants increase their refractive indices. In addition, Eqs. (2) and (3) show that this effect is also translated to the core phase propagation constant and the group delay. Actually, the phase propagation constant variation due to fiber curvatures has been widely studied in many works, [15,16], but there is a lack of investigation on how curvatures affect to the group delay.

The effect of fiber twisting with a constant twist rate $\gamma$ can be understood as a linear rotation of the fiber cross section along a given fiber length $L$; in other words, as a linear increment of the angle $\theta_m$ for a given core $m$. If we applied an ideal curvature with a fixed bending radius over the whole fiber length, the angle $\theta_m$ of each core $m$ would be preserved. The DGD between the outer cores and the central core would then accumulate linearly with the fiber length unless that core $m$ is placed at an angle $\theta = \pi/2 + k\pi$, $k \varepsilon$ Z (where the core belongs to the curvature tangential plane and the DGD is cancelled out). We can denote the longitudinal evolution of the angular coordinate of core $m$ in the cross-sectional area of the fiber as $\theta_m = \theta_{m,i} + \gamma z$, being $z$ the longitudinal coordinate and $\theta_{m,\,i}$ the initial angular position (i.e., when $z = 0$). Thus, for a given core $m$, the DGD with respect to the corresponding straight condition $\tau_m$ is a function of $z$: $DGD(z) = \tau_{eq,m}(z)$ - $\tau_m$. After a given propagation length $L$, the accumulated DGD is given by

$$\begin{aligned} DGD_{accumulated} &= \int_0^L DGD(z)dz \\ &= \frac{1}{c}\int_0^L \left[\frac{1}{\beta_{eq,\,m}}\left(k_0 n_{eq,\,m}^2 - 2\pi n_{eq,\,m}\frac{dn_{eq,\,m}}{d\lambda} + \frac{2\pi}{a_m^2 k_0^2}u_{eq}\frac{du_{eq}}{d\lambda}\right)\right. \\ &\quad \left. - \frac{1}{\beta_m}\left(k_0 n_m^2 - 2\pi n_m\frac{dn_m}{d\lambda} + \frac{2\pi}{a_m^2 k_0^2}u\frac{du}{d\lambda}\right)\right] dz. \end{aligned} \tag{4}$$

In order to find an analytical solution for the accumulated DGD, we can simplify Eq. (4) if we assume that the effective index follows the same equivalent distribution than the refractive index of Eq. (1), which is a consistent approximation under weakly guiding condition. Thus, we can approximate the equivalent effective index of core $m$ as

$$n_{eff_{eq,\,m}} \approx n_{eff}\left(1 + \frac{r_m}{R_b}\cos\theta_m\right). \tag{5}$$

Substituting Eq. (5) into Eq. (3), the equivalent group delay results

$$\tau_{eq,\,m} \approx \tau_m\left(1 + \frac{r_m}{R_b}\cos\theta_m\right), \tag{6}$$

and thus, the DGD with respect to the corresponding straight condition is given by

$$DGD(z) = \tau_{eq,\,m} - \tau_m = \frac{\tau_m r_m}{R_b}\cos(\theta_{m,\,i} + \gamma z), \tag{7}$$

leading to the following analytical expression for Eq. (4):

$$DGD_{accumulated} = \int_0^L DGD(z)dz = \frac{\tau_m r_m}{R_b\gamma}\sin(\theta_{m,\,i} + \gamma L). \tag{8}$$

Optics EXPRESS

For the worst case that gives the maximum value of DGD, i.e. $\theta_{m,\,i} = k\pi$, we have:

$$DGD_{Worst\ case,\ accumulated} = \frac{\tau_m r_m L}{R_b}\mathrm{sinc}(\gamma L)(-1)^k. \tag{9}$$

Figure 2 shows the computed worst-case accumulated DGD for a given core $m$ ($r_m = 35$ μm and $\theta_{m,\,i} = 0$) as a function of the total twist, $\gamma L$, for a fiber length $L = 1$ km under different bent conditions. Solid and dashed lines correspond, respectively, to the worst-case accumulated DGD simulated from Eq. (4) and to the simplified model of Eq. (9). Blue, green and orange lines correspond to a bending radius of 50, 75 and 150 mm, respectively. As shown, both models are in excellent agreement. We see that increasing the bending radius tends to decrease the DGD, as expected. We can observe that the DGD due to fiber curvatures has an important effect on the outer cores that cannot be disregarded, but it decreases rapidly as the twist is increased following a sinc shape, as Eq. (9) suggested. Thus, we can conclude that applying a forced twist helps to reduce the DGD between cores caused by fiber curvatures. Note that the bending radius of $R_b = 75$ mm is the typical radius of optical fiber spools, so that the green curve actually represents typical laboratory measurement conditions.

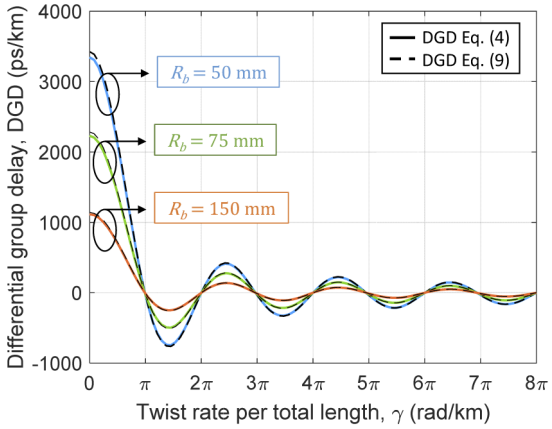


**Fig. 2.** Computed differential group delay (DGD) as a function of the twist rate (rad/km) for a 1-km MCF link and different bending radii ($R_b = 50$, 75, 150 mm), comparing the results from Eqs. (4) and (9).

## 3. Experimental evaluation

We have experimentally evaluated both bending and twisting effects on the DGD of a commercial homogeneous 7-core fiber following the experimental setup illustrated in Fig. 3. The fiber has step-index cores (core radius $a = 4$ μm and core-to-cladding relative index difference $\Delta = 0.31\%$) and a core pitch of 35 μm. We measured the DGDs between straight and bent fiber conditions over a small piece of fiber ($L = 1$ m). This way, we can carry out the straight fiber measurements and properly manage the applied twist while curving the fiber. Small bending radii of 25, 35 and 50 mm (below the typical fiber spool radius) are applied to force a representative variation in the core group delays when the fiber is bent. The fiber is locked with clamps at both ends: before fiber winding, a first clamp holds the fiber at one point, while the second clamp maintains the curvature and twisting conditions after winding.

As Fig. 3 shows, the optical signal coming from a tunable laser is injected into the central core (Core 1) and one of the outer cores (Cores 2-7) of the MCF. Prior to each measurement, we adjusted the optical paths for the central core to have a differential delay of around 20 ps

Optics EXPRESS

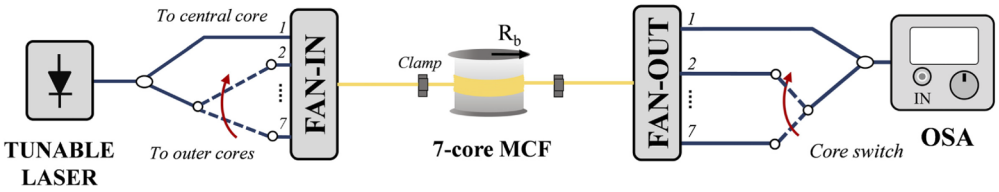


**Fig. 3.** Experimental setup for the measure of the DGD between central and outer cores.

greater than the outer cores. This was done to avoid zero-DGD situations in which the DGD measurement method is not accurate. At the fiber output, both signals are coupled together and injected into an Optical Spectrum Analyzer (OSA). Sweeping the optical wavelength of the laser reveals the interference pattern from which we measure the differential delay between both cores, [17]. As an example, Fig. 4(a) represents the interference pattern of cores 1-2 measured when the fiber is bent at a 25-mm radius within a 10-nm range (from 1545 to 1555 nm). This pattern is then Fourier transformed into the time domain to obtain the temporal representation of Fig. 4(b); the difference between these two peaks determines the DGD due to the curvature.

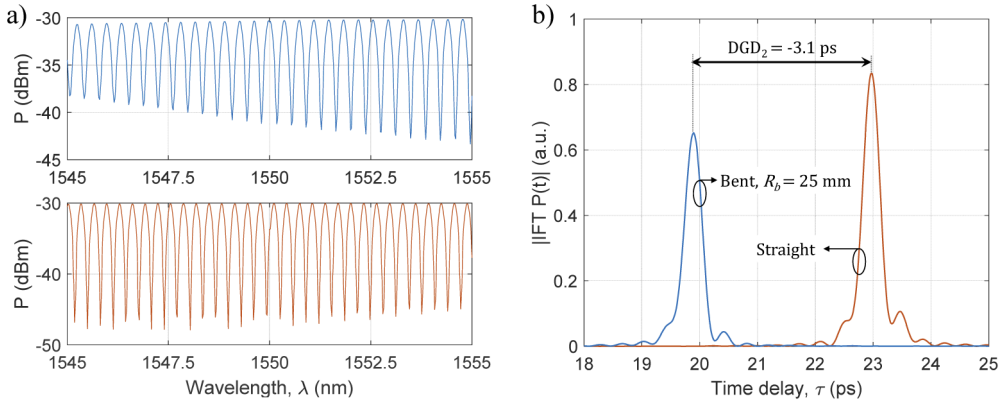


**Fig. 4.** (a) Interference pattern (optical power) measured by the OSA when the fiber is bent at a 25-mm radius (upper) and in straight condition (lower); and (b) temporal waveforms obtained from the inverse Fourier Transform of the interference patterns when the fiber is bent at a 25-mm radius (blue) and in straight condition (orange).

Table 1 gathers the measured DGD values between the outer and central cores for the three bending radii when two different conditions are applied: (a) the fiber is bent among the cylinder carefully trying not to induce any fiber twisting; and (b) the fiber is bent while forcing an intentional twist. For the forced twist experiments, the fiber twisting was manually performed by introducing several intentional rotations distributed along the 1-m fiber while fiber winding. We can see as expected that the DGD is bigger as the bending radius is smaller, as well as how twisting the fiber produces an important reduction on the core DGDs. Slightly asymmetric behavior between the cores with opposite delay variation can be attributed to both fabrication mismatches on the core positions (radial, $r_m$, and angular, $\theta_{m,i}$) with respect to the ideal configuration and also to measurement tolerances.

Figure 5(a) depicts the core DGDs located inside the fiber cross-section for the representative case of $R_b = 35$ mm with and without twist. The position of the tangential plane has been estimated from the core DGD measurements gathered in Table 1. As shown, cores located at one side of the tangential plane have DGDs with opposite signs than those located in the other

Optics EXPRESS

**Table 1. Normalized inter-core DGD (ps/m) values measured between pair of cores for different bending and twisting conditions**

| Cores | No twist | | | Twist | | |
|---|---|---|---|---|---|---|
| | 25 mm | 35 mm | 50 mm | 25 mm | 35 mm | 50 mm |
| 1-2 | −3.1 | −2.0 | −2.7 | −1.0 | −0.8 | −0.7 |
| 1-3 | 2.1 | 1.3 | −0.4 | −0.5 | 0.1 | −0.3 |
| 1-4 | 4.8 | 3.5 | 2.3 | 0.7 | 0.9 | 0.2 |
| 1-5 | 2.2 | 1.9 | 2.4 | 1.0 | 0.1 | 0.0 |
| 1-6 | −2.4 | −1.6 | −0.3 | 0.3 | −0.4 | 0.3 |
| 1-7 | −6.0 | −4.1 | −3.3 | −1.2 | −1.3 | −1.1 |

side. Moreover, the DGD of those cores located in opposite radial positions (i.e., $\theta_{m,i}$ - $\theta_{n,i} = k\pi$) have similar absolute value (ideally identical) but opposite signs. The worst-case DGD variation occurs when the core forms an angle of $\pm\pi/2$ with the tangential plane, but this case cannot actually be measured with precision since we do not have control over the curvature plane (which we assume random) during the measurement process. However, we can estimate the worst-case DGD from the measured values by doing a plane correction. For instance, in the case of the tangential planes of Fig. 5(a), we can apply the plane correction $\theta_c$ (in degrees) that satisfies:

$$\frac{DGD_2}{\cos(60-\theta_c)} = \frac{DGD_7}{\cos(\theta_c)}, \tag{10}$$

being $DGD_2$ and $DGD_7$ the differential group delays of cores 2 and 7, respectively. Once the angle of the plane correction $\theta_c$ is calculated, we can estimate the worst-case DGD as $DGD_{worst-case} = DGD_7/\cos(\theta_c)$. Following an analog procedure, we can estimate the worst-case DGD for each measured case. Figure 5(b) shows the estimated worst-case DGD from the measured values as compared to the theoretical curves obtained from Eqs. (4) and (9), (solid and dashed lines, respectively), when we fix the twist rate to 0. We see that the measured worst-case DGDs in the absence of twist are well-matched with the theoretical curves. On the other hand, we observe an important reduction on the worst-case DGD when an intentional twist is applied while bending the fiber, as expected.

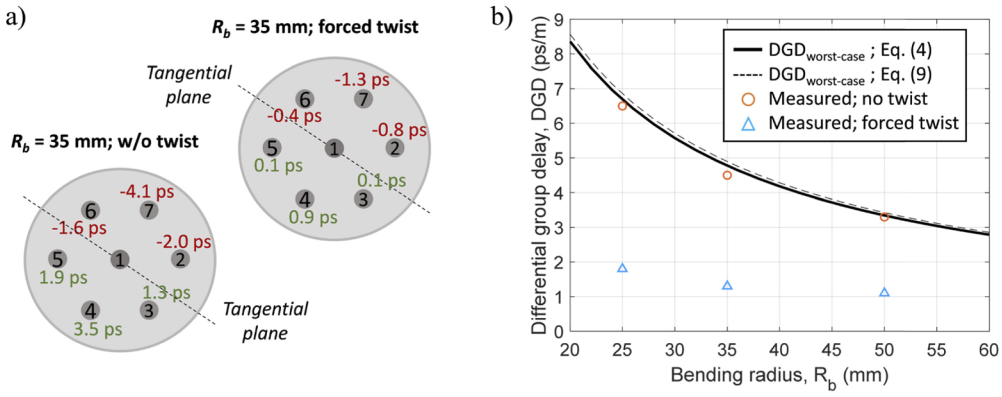


**Fig. 5.** (a) Measured core differential group delays between bent and unbent fiber for a bending radius of 35 mm with and without twist. (b) Differential group delay dependence on the bending radius: Solid and dashed lines correspond to the worst-case computed theoretical responses without twist, while error bars represent the worst-case experimental values (red bars: no twist, blue bars: forced twist).

Optics EXPRESS

## 4. Experimental impact of bending and twisting effects on microwave signal processing applications

Non-desired group delay variations between cores could affect applications where time-delay control and synchronization play a crucial role. This is the case, for instance, of fiber-distributed RF signal processing, where the MCF offers the required parallelism for the compact implementation of a sampled true time delay line architecture using a single optical fiber, [8]. Therefore, we have experimentally evaluated how bending and twisting affect a delay-sensitive application such as Microwave Photonics signal filtering. We implemented a 7-tap finite impulse response filter with a Free Spectral Range of 10 GHz by adjusting the group delay difference between adjacent filter samples (or basic differential delay) to $\Delta\tau = 100$ ps. The filter frequency response was measured for two different fiber conditions: (1) bent without intentional twist and (2) bent with a forced twist, each one for three different bending radii: 25, 35 and 50 mm.

The experimental setup used to measure the filter electrical response is depicted in Fig. 6. This setup was also used in [18], where we presented some preliminary results about this topic. The optical signal is generated by a broadband source (BS) which is then filtered to obtain an optical carrier with a -3-dB bandwidth of 0.3 nm. The use of a BS makes the filter response insensitive to environmental changes such as temperature or vibrations. The optical signal is then modulated and equally launched to all cores using a $1 \times 8$ coupler and a fan-in device. The fiber condition is change for each curvature/twist case similarly to what we did with group delay measurement. At each fanout output, 2 cm of singlemode fiber (approximately 100-ps delay) were added incrementally from tap to tap to obtain the basic differential delay. A series of variable delay lines (VDLs) at the output of the MCF were used to finely tune the tap delays. To obtain a uniform amplitude distribution between the filter taps, we used Variable Optical Attenuators (VOAs). Output signals are combined before photodetection. The electrical response is measured by a Vectorial Network Analyzer (VNA), which also generates the RF input signal.

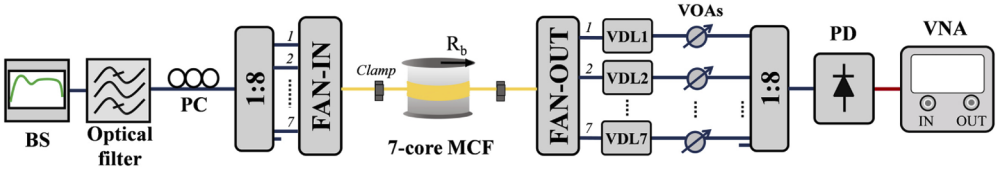


**Fig. 6.** Setup scheme for the experimental measure of MWP signal filtering response.

Figure 7 illustrates the measured filter transfer function as a function of the RF frequency for the different bending/twisting cases stated before. The blue solid line represents the case in which the fiber is wound over the cylinder with a forced regular twist and the red dash-dotted line represents the case where the fiber is bent trying not to produce any twist. In the absence of twist, the filter response when the fiber is bent at 25 mm (Fig. 7(a)) experiences distortions even in the first resonance. When the curvature radius is 35 mm (Fig. 7(b)), the distortions are less important but still present at high frequency resonances. Finally, in the last case (Fig. 7(c)), distortions only appear importantly at the last resonance represented. In all cases, the filter response greatly improves when the intentional twist is applied due to the reduction in the DGDs between cores, as we have seen in section 3. This is particularly important for high-frequency resonances where bent-induced DGD deviations have greater effect on the RF response. These results show how applying a moderate twist to the fiber helps reducing the DGD variations introduced by the fiber itself and, thus, improve the performance of the implemented signal processing functionality.

Optics EXPRESS

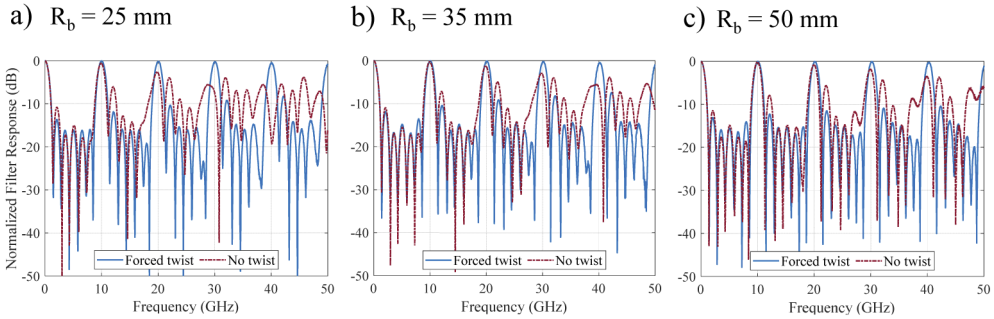


**Fig. 7.** Measured filter response for: (solid blue) fiber bent with high twist, (dash-dotted red) fiber bent with low twist; and different radius: a) 25 mm b) 35 mm c) 50 mm.

## 5. Conclusions

One of the most important sources of degradation that could compromise the performance of time-delay sensitive applications that incorporate MCFs relates to possible bending and twisting effects. In this paper, we have evaluated both theoretically and experimentally how fiber bending and twisting induce group delay variations between the central and outer cores of an MCF. We have obtained analytical expressions for the computation of the bend-induced DGD accumulated on a given fiber length for a constant twist rate. We must note that the effect of the fiber twist on the intercore DGD has been evaluated in terms of the linear rotation of the fiber cross-section area along the fiber. However, we have not considered the effect of twist-induced birefringence caused by possible deformations in the ellipticity of the cores as a consequence of the applied torsional strain, [19].

Experimental comparison of the effect of different twisting conditions was carried on a 1-m link of homogeneous 7-core MCF for three different bending radii of 25, 35 and 50 mm. These effects were also evaluated experimentally in the context of a particular time-sensitive scenario, time-discrete microwave signal filtering, where the 7 cores acted as the optical carriers for the 7 filter taps. Our results for RF frequencies up to 50 GHz show how even a tightly bent 1-m MCF can degrade the performance of this application and how fiber twisting is actually beneficial to counteract the group delay variations produced by the fiber curvature. These findings are generally applicable to time-delay sensitive application areas such as radio-over-fiber distribution and MWP signal processing in fiber-wireless access networks, as well as high-capacity long-haul digital communications where digital MIMO processing may be required.

## Funding

European Research Council (Consolidator Grant 724663); Spanish Ministerio de Economía y Competitividad (BES-2015-073359 for S. Garcia, RYC-2014-16247 for I. Gasulla, TEC2016-80150-R).

## References

1. D. J. Richardson, J. M. Fini, and L. E. Nelson, "Space-division multiplexing in optical fibers," Nat. Photonics **7**(5), 354–362 (2013).
2. D. Barrera, I. Gasulla, and S. Sales, "Multipoint two-dimensional curvature optical fiber sensor based on a non-twisted homogeneous four-core fiber," J. Lightwave Technol. **33**(12), 2445–2450 (2015).
3. J. Capmany, J. Mora, I. Gasulla, J. Sancho, J. Lloret, and S. Sales, "Microwave photonic signal processing," J. Lightwave Technol. **31**(4), 571–586 (2013).
4. T. Hayashi, T. Nagashima, O. Shimakawa, T. Sasaki, and E. Sasaoka, "Crosstalk variation of multi-core fibre due to fibre bend," in *Proceedings of 36th European Conference and Exhibition on Optical Communication*, Torino, 2010, pp. 1–3.

Optics EXPRESS


5. T. Hayashi, T. Sasaki, E. Sasaoka, K. Saitoh, and M. Koshiba, "Physical interpretation of intercore crosstalk in multicore fiber: effects of macrobend, structure fluctuation, and microbend," Opt. Express **21**(5), 5401–5412 (2013).
6. A. A. Nasir, S. Durrani, and R. A. Kennedy, "Blind timing and carrier synchronisation in distributed multiple input multiple output communication systems," IET Communications **5**(7), 1028–1037 (2011).
7. J. M. Galve, I. Gasulla, S. Sales, and J. Capmany, "Reconfigurable radio access networks using multicore fibers," IEEE J. Quantum Electron. **52**(1), 1–7 (2016).
8. I. Gasulla and J. Capmany, "Microwave photonics applications of multicore fibers," IEEE Photonics J. **4**(3), 877–888 (2012).
9. S. García and I. Gasulla, "Dispersion-engineered multicore fibers for distributed radiofrequency signal processing," Opt. Express **24**(18), 20641–20654 (2016).
10. S. Garcia and I. Gasulla, "Experimental demonstration of multi-cavity optoelectronic oscillation over a multicore fiber," Opt. Express **25**(20), 23663–23668 (2017).
11. T. Sakamoto, T. Mori, M. Wada, T. Yamamoto, T. Matsui, K. Nakajima, and F. Yamamoto, "Experimental and numerical evaluation of inter-core differential mode delay characteristic of weakly-coupled multi-core fiber," Opt. Express **22**(26), 31966–31976 (2014).
12. D. Marcuse, "Influence of curvature on the losses of doubly clad fibers," Appl. Opt. **21**(23), 4208–4213 (1982).
13. D. Gloge, "Weakly guiding fibers," Appl. Opt. **10**(10), 2252–2258 (1971).
14. S. Garcia and I. Gasulla, "Universal characteristic equation for multi-layer optical fibers," submitted to Opt. Express (2019).
15. M. Koshiba, K. Saitoh, K. Takenaga, and S. Matsuo, "Multi-core fiber design and analysis: coupled-mode theory and coupled-power theory," Opt. Express **19**(26), B102–B111 (2011).
16. M. Koshiba, K. Saitoh, K. Takenaga, and S. Matsuo, "Analytical expression of average power-coupling coefficients for estimating intercore crosstalk in multicore fibers," IEEE Photonics J. **4**(5), 1987–1995 (2012).
17. C. Dorrer, N. Belabas, J. P. Likforman, and M. Joffre, "Spectral resolution and sampling issues in Fourier-transform spectral interferometry," J. Opt. Soc. Am. B **17**(10), 1795–1802 (2000).
18. S. García, M. Ureña, R. Guillem, and I. Gasulla, "Multicore fiber delay line performance against bending and twisting effects," in *Proceedings of 2018 European Conference on Optical Communication (ECOC)*, Rome, 2018, pp. 1–3.
19. A. M. Smith, "Birefringence induced by bends and twists in single-mode optical fiber," Appl. Opt. **19**(15), 2606–2611 (1980).